Finite element simulation of the high-strain dynamic test and the static load test performed on the test pile of the George Massey Tunnel Replacement project

Juan-Carlos Carvajal [i)] and David Tara [i)]

i) Senior Geotechnical Engineer, Thurber Engineering, 900 - 1281 West Georgia Street, Vancouver, Canada.

ABSTRACT

High-strain dynamic and static loading tests were performed on a 2.0 m diameter, 67 m embedment, open-toe, steel pipe pile driven in a deltaic deposit comprised of compact sand and stiff clayey silt. Dynamic tests were carried out at 1 day, 7 days, and 29 days after pile installation, and a static test at 80 days after pile installation. Axisymmetric finite element analyses were performed with PLAXIS2D to determine the soil properties that control the shaft and the toe resistance of the pile using both dynamic and static load testing data. The geotechnical properties of the PLAXIS model were obtained by matching the work time history in the time interval of maximum energy transfer with that obtained from the dynamic test. The analysis indicates that the estimation of the pile resistance using high-strain dynamic testing is mainly associated with the shaft resistance due to the very small mobilization of the toe displacement during the dynamic test. The ultimate geotechnical resistance is obtained by simulating a static load test with the calibrated PLAXIS model with a pile head displacement equal to 200 mm, which is equivalent to 10% of the pile diameter.

Keywords: displacement, shaft resistance, toe resistance, work time history

1 INTRODUCTION

The geotechnical axial resistance of driven steel pipe piles is commonly obtained with high-strain dynamic testing by measuring the acceleration and the strain in the pile caused by an impact of the driving hammer (ASTM D4945-17). The resistance is determined by matching the measured pile response with that calculated using one-dimensional wave equation analysis (1D WEA), implemented in commercial software.

High-strain dynamic testing is significantly cheaper and faster than static load testing. However, the sensitivity of the matching procedure and the small pile displacement mobilized in the dynamic test can result in underestimation of the geotechnical pile resistance in comparison to that obtained with static load testing, which could significantly affect the foundation cost. In addition, the analyst's experience is a dominant factor in the estimation of the pile resistance with 1D WEA.

This paper describes a simple yet robust procedure for estimating the geotechnical axial resistance of open-toe, driven steel pipe piles using high-strain dynamic testing and finite element analysis. The procedure is validated with both static and high-strain dynamic load tests performed on a large pile diameter installed for the George Massey Tunnel Replacement Project. The pile resistance obtained with the proposed procedure is compared to that obtained with the signal matching software CAPWAP (Case Pile Wave Analysis Program), which is based on 1D WEA.

2 SITE CONDITIONS AND PILE DIMENSIONS

The test pile site is located on the floodplain of the south arm of the Fraser River in the City of Delta, British Columbia, Canada. The subsurface conditions consist of compact sand to 22 m depth, soft to very stiff clayey silt to 52 m depth, compact to dense sand to 71 m depth, firm to stiff silty clay / clayey silt to 123 m depth, and a sequence of the very stiff silty clay and very dense sand layers to about 300 m depth, followed by very dense Glacial till. The ground water table (gwt) is at about 1.0 m to 2.0 m depth.

Four 2.0 m diameter by 24.3 mm thick reaction piles (RP1 to RP4), and one 2.0 m diameter by 30.7 mm thick test pile (TP) were installed to about 67 m depth between March 12 and May 31, 2016. The piles consisted of ASTM A252 Grade 3 pipes welded in 11.9 m long sections and driven open toe with an APE D180-42 diesel hammer.

The average peak friction angle (ϕ) of the sandy layers, the average plasticity index (PI) of the clayey layers, and the average shear wave velocity of the soil deposit in the upper 75 m is $\phi \approx 35°$, PI $\approx$ 10%, and

$V_s \approx 250$ m/s, respectively.

3 FINITE ELEMENT MODEL

The numerical simulation of the static and dynamic pile load tests is carried out with an axisymmetric finite element (FE) model using PLAXIS2D. The components, dimensions, and boundary conditions of the model are shown in Figure 1.

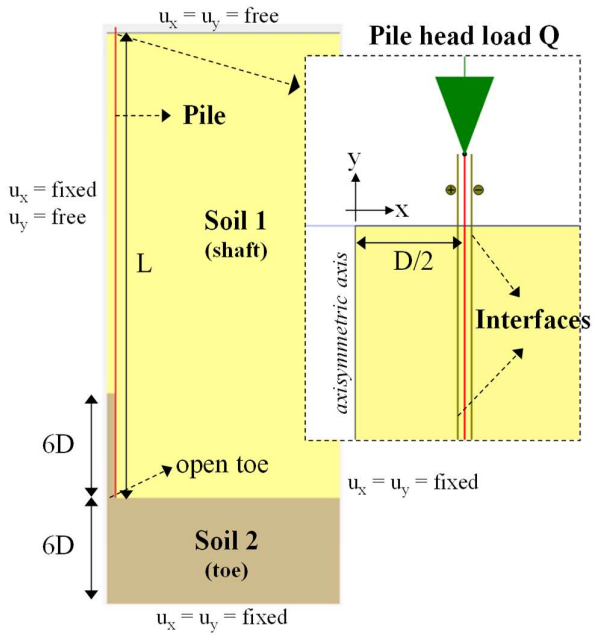

Fig. 1. Axisymmetric finite element model for simulating the static and dynamic axial response of an open-toe, steel pipe pile.

The pile is modeled with an elastic plate element located at x = D/2 from the axisymmetric axis and with embedment L, where D is the pile diameter. The pile projection above ground surface is 0.7 m. The input parameters (per meter of perimeter) are the axial stiffness EA (kN/m), the bending stiffness EI (kN·m^2/m), the pile weight w = γ t (kN/m/m), and Poisson's ratio ν = 0.3. In the above parameters, t is the wall thickness, E = 2x10^8 kPa is the Young's modulus of steel, A = t is the unit pile cross-section area, I = t^3/12 is the unit second moment of inertia, and γ = 77 kN/m^3 is the unit weight of steel. Interfaces are added inside and outside of the plate element for modeling the shaft-soil interaction and extended below the pile toe a distance equal to the maximum pile head displacement in the static load test plus 50 mm.

The shear modulus G_{inter} and the effective friction angle ϕ_{inter} of the shaft-soil interface (inside and outside) is calculated in PLAXIS2D with the interface strength reduction factor (R_{inter}), which is an input parameter of the adjacent soil material $\rightarrow G_{inter} = (R_{inter})^2 G_{soil}$ and $\phi_{inter} = \tan^{-1}[R_{inter} \tan(\phi_{soil})]$. Gap closure was considered in the interface formulation.

The soil was modeled with the Mohr-Coulomb model, for which input parameters are the soil unit weight γ_{soil} = 19 kN/m^3, Poisson's ratio ν = 0.25, effective cohesion c = 1 kPa (for numerical stability), effective peak friction angle ϕ, dilation angle $\psi = 0°$, and the shear wave velocity V_s, which is used as an alternate input parameter for calculating the Young's modulus E_{soil} and the shear modulus G_{soil}.

The soil conditions along the embedded portion of the pile and below the toe consist of several layers of loose to dense sand and soft to very stiff clayey silt, for which the geotechnical properties can be defined in terms of drained or undrained strength.

For simplicity in the determination of the shaft and the toe resistance using the pile test data, the FE model is divided into only two soil layers: Soil 1 and Soil 2 with shear strength given by the peak friction angle (ϕ). Soil 1 represents the soil above the pile toe and controls the shaft resistance. Soil 2 is located below the pile toe with a total thickness of 6D and controls the toe resistance. Soil 2 is extended upward a distance of 6D inside the pile to differentiate the properties of the soil contributing to the outside shaft resistance from the inside resistance. This is what controls the toe response of an open toe pipe pile. The 6D dimensions were determined with a sensitivity analysis of simulations of static load tests. The total width of the model is 25 m and the gwt is at ground surface.

4 SIMULATION OF STATIC LOAD TESTS

The static load test on the test pile was carried out on August 18, 2016, which represents about 80 days after pile installation. The static test included removal of the soil and placement of concrete infill in the upper 20 m of the test pile.

Simulation of the static load test is carried out with a displacement-based pushover analysis. The pile head is pushed downwards up to a given target displacement and the unit axial force (kN/m) is extracted from the closest stress point to the pile head. The load-displacement response of the pile head is calculated by multiplying the output unit force with the pile perimeter Per = πD.

The analysis is divided in five phases of plastic analyses: a) initiation of the in-situ stresses using the K_o procedure, b) activation of the plate element (the pile) and the interfaces, c) removal of soil and placement of the concrete infill in the upper 20 m of the pile, d) application of the target displacement $\rightarrow$ loading stage, and e) deactivation of the target displacement $\rightarrow$ unloading stage. The analysis assumes "wished in place" conditions, so no pile installation effects such as soil plug development or residual stresses are considered directly.

The objective of the simulation of the static load test is to determine the properties of the shaft-soil interfaces and the Soil 2 (toe) material that better match the measured load-displacement pile response. Therefore, a calibration procedure is carried out by varying the

following three input parameters: R_{inter} (same for Soil 1 and Soil 2), and ϕ_{toe} and V_{s_toe} of Soil 2. The properties of the Soil 1 (shaft) material are kept constant (ϕ = 35°, V_s = 250 m/s) since the pile-shaft resistance is controlled by R_{inter}.

The diameter, wall thickness and embedment of the test pile are 2000 mm, 30.7 mm, and 67.0 m, respectively. The 20 m concrete infill was modeled as an elastic material with unit weight γ = 24 kN/m^3 and shear wave velocity $V_s \approx$ 2450 m/s. Rigid interface condition was assumed between the concrete infill and the test pile $\rightarrow R_{inter} = 1$.

Figure 2 shows the pile head response (Q-U) measured with the static load test and that simulated with PLAXIS for a maximum pile head displacement of 295 mm, where Q is the pile head load and U is the pile head displacement. The pile toe displacement is also plotted for visualization/confirmation of the full mobilization of the shaft resistance (Q_{shaft}) and the mobilization of the toe resistance (Q_{toe}).

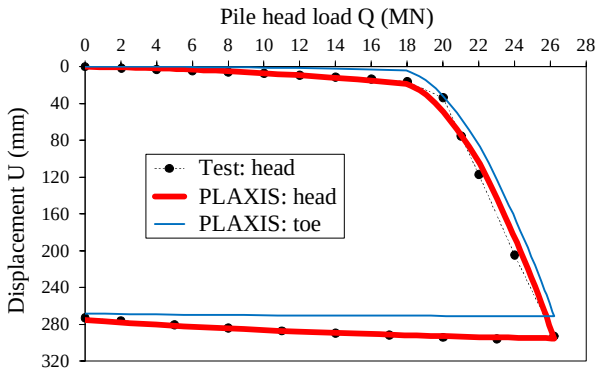

Fig. 2. Simulation of the static load test on the test pile (TP): 2.0 m Diameter x 67 m embedment.

Figure 2 shows that the pile head response simulated with the two-layer, axisymmetric, Mohr-Coulomb, finite element model (PLAXIS) matches reasonably well the pile response measured with the static load test for both the loading and the unloading stages. The calibrated soil properties of the PLAXIS model are:

- R_{inter} = 0.41, ϕ_{toe} = 22°, V_{s_toe} = 150 m/s

The friction angle of the shaft-soil interfaces (obtained from R_{inter}) for Soil 1 (inside and outside the pile) is $\phi_{inter} \approx$ 16°, and for Soil 2 (inside the pile) is $\phi_{inter} \approx$ 9.4°. The shear strength of the interfaces is not only controlled by ϕ_{inter} but also by the vertical and the horizontal stresses, which increase in the Soil 2 interface with the at-rest earth pressure coefficient, $K_o = 1 - \sin(\phi_{toe})$, and the pile toe displacement.

The pile head and pile toe responses in Figure 2 clearly show the pile head load (Q_{shaft}) and the associated pile head displacement (U_{shaft}) for full mobilization of the geotechnical shaft resistance:

- $Q_{shaft} \approx$ 18.4 MN and $U_{shaft} \approx$ 20 mm

For $Q > Q_{shaft}$, the total geotechnical axial resistance ($Q = Q_{shaft} + Q_{toe}$) is controlled by the toe displacement and the associated toe resistance Q_{toe}. For the maximum pile head displacement of 295 mm in the static load test, the pile resistance is:

- $Q_{shaft} \approx$ 18.4 MN + $Q_{toe} \approx$ 7.8 MN = $Q \approx$ 26.2 MN

Figure 3 plots the contour plots of the effective vertical stress (a) and the deviatoric stress (b) in the soil located in the lower 12 m of the test pile at the end of the loading stage for a pile head displacement of U_{head} = 295 mm, which is the maximum displacement in the static load test. The red and dark blue colors represent maximum and minimum stress, respectively.

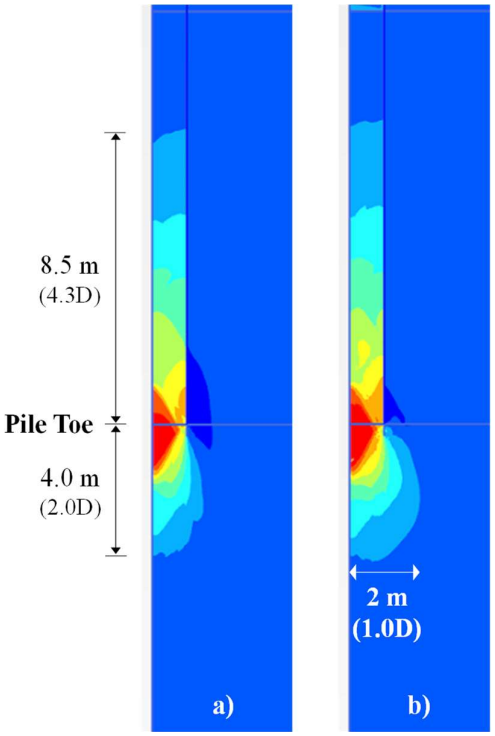

Fig. 3. Contour plot of the a) effective vertical stress and b) the deviatoric stress in the soil for a pile head displacement of 295 mm in the static load test.

Figure 3 shows a stress concentration inside the pile that extends up to about 8.5 m above the pile toe. Below the pile toe, the stress concentration extends up to about 4 m in the vertical direction and 2 m in the horizontal direction, which represents a stress bulb below the pile toe with approximated dimensions of 2D x 2D, where D is the pile diameter. The stress bulb below the pile toe determines the resistance and displacement of the toe and depends on the inside shaft resistance.

Figure 4 shows the mobilized shear stress along the inside interface of the pile at the end of the loading stage of the static load test for 295 mm of pile head displacement.

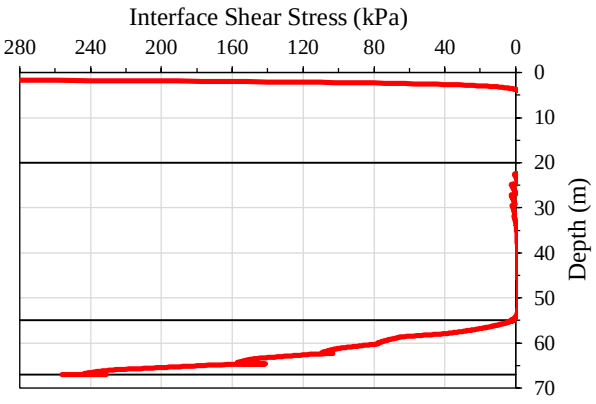

Fig. 4. Mobilized shear stress along the inside interface of the test pile (TP) for a head displacement of 295 mm in the static load test.

The maximum interface shear stress inside the pile is about 260 kPa at the pile toe (67 m depth) and it decreases gradually to about 0 kPa at 12 m above the pile toe (55 m depth) as shown in Figure 4. From 20 m to 55 m depth, the mobilized shear stress is about zero. From 0 to 20 m depth, the interface shear stress is also zero but with strong stress concentrations of opposite directions (±5,000 kPa) at the ends of the concrete infill (at 0 m and at 20 m depth) because of the rigid interface assumption between the concrete and the pile. The inside shaft resistance from 55 m to 67 m depth is $Q_{shaft\_inside} \approx$ 7.8 MN, which is equal to the toe resistance obtained from the static load test for 295 mm of pile head displacement.

The lack of mobilization of interface shear stress from about 0 m to 55 m depth inside the pile is due to the zero relative displacement in the interface between the inner concrete/soil core and the pile shaft. Therefore, the concrete/soil core moves downwards with the pile with negligible shear resistance, except in the lower 12 m of the pile.

The effective-stress proportionality coefficient (Bjerrum-Burland coefficient) of the outside shaft-soil interface is $\beta \approx 0.14$, which is calculated as $\beta = Q_{shaft} / (0.5\ \gamma'\ \pi D\ L^2)$, where $Q_{shaft} \approx 18.4$ MN, $\gamma' = 9.2$ kN/m^3 is the submerged soil unit weight, D = 2 m is the pile diameter, and L = 67 m is the pile embedment.

5 LOAD VS DISPLACEMENT EQUATIONS

The static load test results show that the response of the pile head is characterized by three loading regions that depend on the pile head displacement: a) the shaft response, b) the toe response, and c) unloading, as shown in Figure 5.

Equations 1, 2 and 3 represent proposed formulations (quadratic functions) for calculating the pile head response (Q-U) for the shaft, the toe, and the unloading regions of the static load test, respectively.

$$U = (U_{shaft} - C_{shaft})\ [Q/Q_{shaft}] + C_{shaft}\ [Q/Q_{shaft}]^2 \quad (1)$$

$$U = U_{shaft} + B_{toe}\ [Q/Q_{shaft} - 1] + C_{toe}\ [Q/Q_{shaft} - 1]^2 \quad (2)$$

$$U = U_{max} + B_{unload}\ [Q/Q_{max} - 1] + C_{unload}\ [Q/Q_{max} - 1]^2 \quad (3)$$

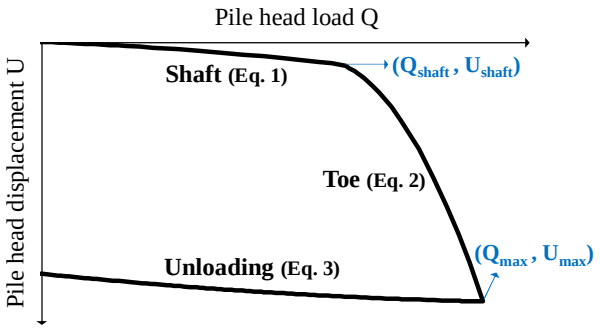

Fig. 5. Loading regions in a static load test of an open-toe, steel pipe pile embedded in a deltaic deposit.

In the above equations, U_{shaft} and Q_{shaft} are the pile head displacement and pile head load that represent the full mobilization of the shaft resistance, and U_{max} is the maximum pile head displacement associated with the maximum pile head load Q_{max} in the static load test, as shown in Figure 5. The remaining parameters C_{shaft}, B_{toe}, C_{toe}, B_{unload}, and C_{unload} control the curvature of the Q-U response. The parameters are determined with an error minimization procedure using either the static load test data or the PLAXIS data of the Q-U pile head response.

The proposed Q-U equations can be implemented in a spreadsheet to facilitate the estimation of the geotechnical pile resistance for a given target pile head displacement or geotechnical resistance factor (ϕ_{gu}).

Figure 6 plots the Q-U pile head response using Eqs. 1 to 3 (black line). The parameters were obtained using the PLAXIS data (red line) and the function "solver" included in Microsoft Excel.

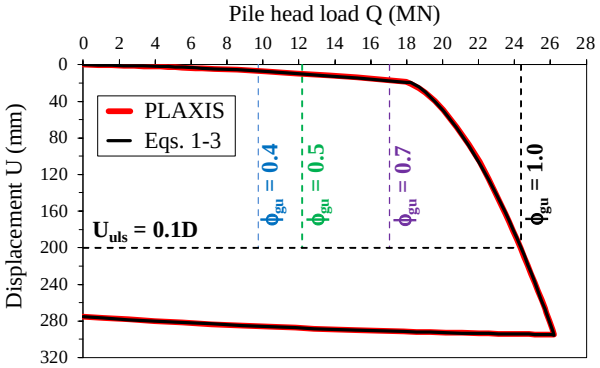

Fig. 6. Curve fitting of the static load test on the test pile

As shown in Figure 6, the proposed equations match very well the simulation of the static load test with PLAXIS for the loading and unloading regions.

The geotechnical ultimate limit state axial resistance of a pile is associated with a target displacement, which is project dependent and normally taken as U_{uls} = 5% to 15% of the pile diameter D. For this study, the

geotechnical ultimate axial resistance (Q_{uls}) is calculated for U_{uls} = 0.1D using the Q-U curve in Figure 6:

- Q_{uls} = 24.35 MN for U_{uls} = 200 mm, where Q_{shaft} = 18.42 MN and Q_{toe} = 5.93 MN

The geotechnical resistance factor for calculation of the factored axial resistance is ϕ_{gu} = 0.7 if the design is based on a static load test (CSA S6-19). Therefore, the factored resistance ($\Phi Q_{uls} = \phi_{gu} Q_{uls}$) and the associated pile head displacement ($U_{0.7}$) are:

- $\Phi Q_{uls} \approx$ 17 MN for $U_{0.7} \approx$ 17.5 mm

As shown in Figure 6, the displacement of the pile head associated with a geotechnical resistance factor ϕ_{gu} = 0.7 is less than 20 mm and therefore it is in the loading region entirely controlled by the shaft resistance.

For a design based on high-strain dynamic testing (ϕ_{gu} = 0.5) or static analysis (ϕ_{gu} = 0.4) with typical degree of understanding of the soil conditions (CSA S6-19), the pile head response is in the loading region controlled by the shaft resistance with associated pile head displacements less than 10 mm, approximately.

6 SIMULATION OF DYNAMIC LOAD TESTS

The simulation of the high-strain dynamic load test is carried out with a force-based pushover analysis. The pile head is pushed downwards with the force time history measured in the dynamic test and the displacement time history is extracted from the closest node to the pile head. The input force for the axisymmetric analysis is calculated as $P_{axi} = P_{test} / 2\pi$, where P_{test} is calculated as the product of E_{steel} and the axial strain time history measured in the dynamic test.

The dynamic analysis is divided in three phases: a) initiation of the in-situ stresses using the K_o procedure, b) activation of the plate element and the interfaces, and c) application of the input force time history. The analysis assumes "wished in place" conditions. The dynamic control parameters are α = 0.25, β = 0.50, and mass matrix = 1.

The objective of the simulation of the high-strain dynamic load test is to determine the properties of the shaft-soil interfaces and the Soil 2 material (toe) that better match the work time history $W_{(t)}$ of the pile head, obtained from the dynamic test data.

$W_{(t)}$ is calculated as the product of the pile head force (P) and the pile head displacement (U) as shown in Equation 4, where the subindexes i and t represent the dynamic time.

$$W_{(t)} = \Sigma \Delta W_i \rightarrow \Delta W_i = \tfrac{1}{2} [P_i + P_{i+1}][U_{i+1} - U_i] \qquad (4)$$

High-strain dynamic analyses are strongly dependent on the viscoelastic damping (energy dissipation) of the pile and the soil. This is modeled in PLAXIS with Rayleigh damping, for which input parameters are two frequencies of vibration (F_1, F_2) and two associated damping ratio values (ξ_1, ξ_2).

Based on sensitivity and parametric analyses carried out for this study, it was determined that the frequencies of vibration for both soil and pile are F_1 = c/4L (the fundamental frequency of vibration of the pile) and F_2 = 1000 Hz, where $c = (E_{steel}/\rho_{steel})^{0.5}$ = 5,048 m/s is the velocity of the axial wave in the pile and L is the sum of the pile embedment and the pile projection. F_2 = 1000 Hz makes the dynamic response less dependent on the stiffness and more dependent on the mass of the materials (i.e., pile and soil).

The viscoelastic damping ratio is assumed to be equal for both frequencies ($\xi = \xi_1 = \xi_2$), and for the pile and the soil materials $\rightarrow \xi = \xi_{soil} = \xi_{pile}$. Therefore, ξ represents the viscoelastic energy dissipation of the entire system: pile + soil + interfaces. Additional energy dissipation is developed in the FE model due to hysteretic damping. This is caused by the full mobilization of the shear strength of the shaft-soil interfaces. The last source of energy dissipation in the FE model is the radiation damping, which is caused by the propagation of the shear and compression waves generated at the pile shaft and pile toe, respectively, during the dynamic test.

The matching of the work time history of the pile head is carried out between the dynamic times t_o and t_{max}, where t_o is the initial impact of the hammer and t_{max} is the time of the maximum work but not greater than $t_2 = t_o + 2L/c$, which is the theoretical arrival time of the axial wave in the pile returning from the toe:

$$t_o \leq \text{time interval for matching} \leq t_{max} \leq t_2 \qquad (5)$$

Figure 7 plots, for instance, the work time history of the pile head obtained from the high-strain dynamic test performed on the test pile (TP) for Beginning of Restrike (BOR) at 1 day after final pile installation.

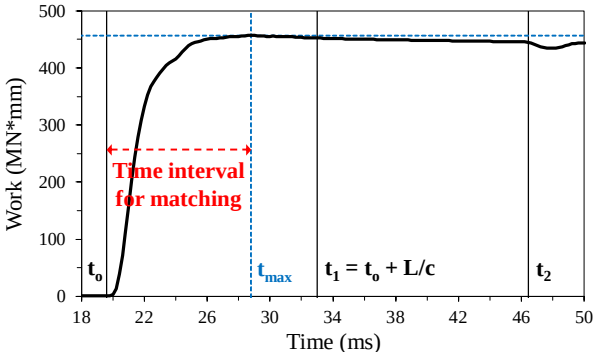

Fig. 7. Work time history of Test Pile (TP) BOR – Day 1.

As shown in Figure 7, the hammer impact occurs at t_o = 19.6 ms and the maximum work occurs at t_{max} = 28.8 ms. These two times mark the time interval for matching the work time history. Two additional time markers are indicated in Figure 7: t_1 and t_2, which represent the time when the longitudinal wave arrives at the toe and at the head (returning wave) of the pile, respectively. As shown in Figure 7, the maximum work occurs before t_1 for this relatively long pile (67 m

embedment) driven with a diesel hammer. However, this is not necessarily the same situation for shorter piles driven with a hydraulic hammer, in which the maximum work occurs between t_1 and t_2 or at t_2 (Carvajal and Tara 2022a).

Figure 8 plots the power time history of the pile head for Test Pile BOR – Day 1, obtained as the variation of the work time history per sampling time increment → $Power_{t+1} = (Work_{t+1} – Work_t) / \Delta t$, where $\Delta t = 0.2$ ms is the sampling time increment.

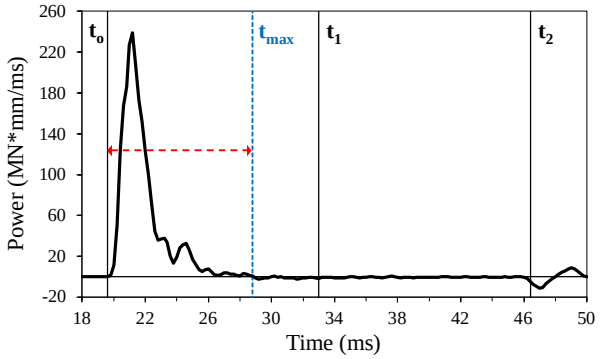

Fig. 8. Power time history of Test Pile BOR – Day 1.

As shown in Figure 8, most of the strain energy transferred from the hammer to the pile head occurs between about 20 ms and 25 ms, with a very minor contribution from 25 ms to 28.8 ms (t_{max}). The power is practically zero from 28.8 ms up to about 46 ms (t_2), where a small oscillation in the power occurs due to the longitudinal wave returning from the toe.

Figure 9 plots the force time history recorded at Test Pile (TP) BOR – Day 1. As shown in the figure, the power time history and the force time history are relatively similar in shape with their maximum values occurring at about 21 ms.

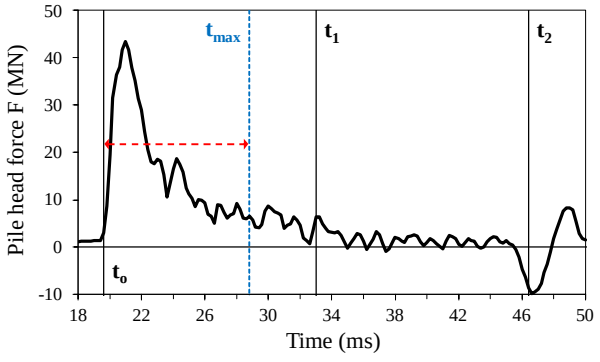

Fig. 9. Force time history of Test Pile BOR – Day 1.

The calibration of the FE model is carried out by varying R_{inter} (same for Soil 1 and Soil 2), ϕ_{toe} and V_{s_toe} of Soil 2, and ξ (same for the pile, Soil 1, and Soil 2). The properties of Soil 1 are kept constant ($\phi = 35°$, $V_s = 250$ m/s).

6.1 Matched work time history

Figures 10, 11, and 12 plot the work time histories obtained from the high-strain dynamic test and from the calibrated PLAXIS finite element model in the time interval of interest (t_o - t_{max}) for the Test Pile (TP) BOR – Day 1, Test Pile (TP) BOR – Day 7, and the Reaction Pile 3 (RP3) BOR – Day 29, respectively.

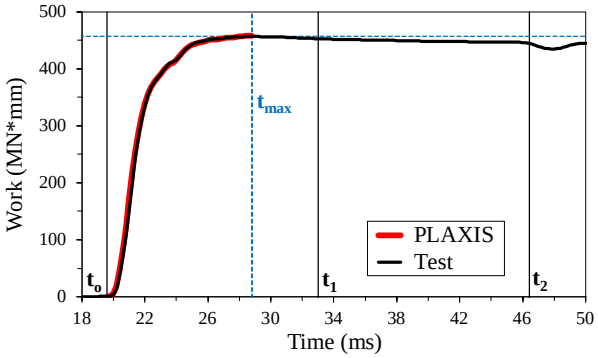

Fig. 10. Work time history of the Test Pile (TP) BOR – Day 1.

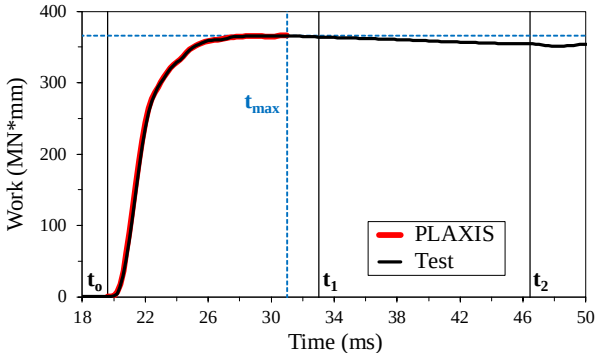

Fig. 11. Work time history of the Test Pile (TP) BOR – Day 7.

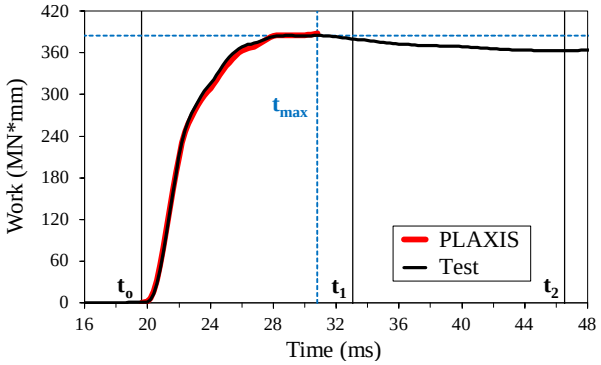

Fig. 12. Work time history of the Reaction Pile 3 (RP3) BOR – Day 29.

As shown in Figures 10 to 12, the match of the work time histories between the dynamic test and the PLAXIS model in the time interval of interest (t_o - t_{max}) is good. The calibrated soil properties of the PLAXIS models are:

- TP BOR-Day 1: $R_{inter} = 0.20$, $\xi = 19\%$
- TP BOR-Day 7: $R_{inter} = 0.29$, $\xi = 18\%$

- RP3 BOR-Day 29: $R_{inter} = 0.31$, $\xi = 16\%$

The associated friction angles of the shaft-soil interfaces (obtained from R_{inter}) for Soil 1 (outside interface for shaft resistance) and Soil 2 (inside interface for toe resistance) are:

- TP BOR-Day 1: shaft $\phi_{inter} = 8.0°$, toe $\phi_{inter} = 4.6°$
- TP BOR-Day 7: shaft $\phi_{inter} = 11.5°$, toe $\phi_{inter} = 6.7°$
- RP3 BOR-Day 29: shaft $\phi_{inter} = 12.2°$, toe $\phi_{inter} = 7.1°$

The interface strength reduction factors (R_{inter}) and the associated interface friction angles (ϕ_{inter}) obtained from the high-strain dynamic test data and the PLAXIS models indicate a gradual increase of the shaft-soil interface strength (outside and inside) with time, which is due to soil setup. The maximum interface strength reduction factor is for RP3 BOR – Day 29 → R_{inter} = 0.31, which is about 75% of that obtained from the static load test data carried out 80 days after pile installation → R_{inter} = 0.41.

The calibration of the PLAXIS models indicated that the dynamic response of the pile is practically insensitive to the properties of the Soil 2 material (ϕ_{toe}, V_{s_toe}) for the three high-strain dynamic tests. This is likely due to the very small displacements induced in the pile toe during the dynamic test (< 9 mm), especially in the time interval of interest ($t_o - t_{max}$) → $U_{toe} \approx 0$ mm, as shown in Figure 13.

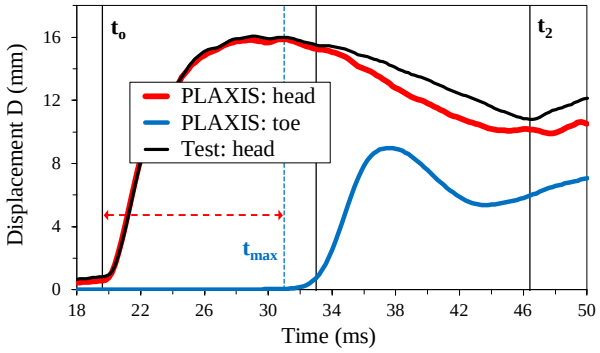

Fig. 13. Displacement time history of TP BOR – Day 7.

Therefore, it is concluded that the pile resistance obtained from the simulation of the high-strain dynamic test with PLAXIS represents mainly the shaft resistance due to the small displacement of the pile head and the pile toe mobilized during the test. Because of the limitation of the mobilized pile displacement in the dynamic test, the soil properties of the toe material (ϕ_{toe}, V_{s_toe}) cannot be accurately determined for the three dynamic tests.

6.2 Pile head force vs displacement

Figures 14, 15 and 16 plot the force versus displacement response of the pile head during the high-strain dynamic test for TP BOR - Day 1, TP BOR - Day 7, and RP3 BOR – Day 29, respectively, for the time interval of interest ($t_o - t_{max}$). As shown in the figures, the simulation of the high-strain dynamic test with the PLAXIS model agrees reasonably well with the dynamic test data.

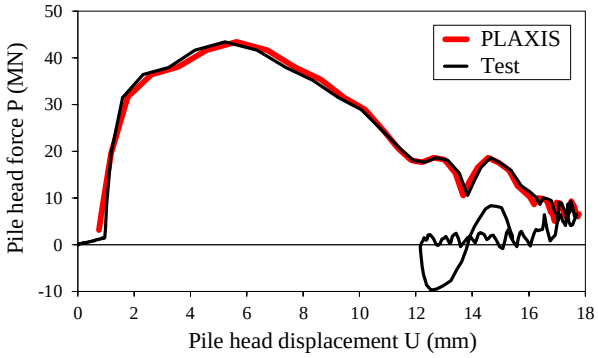

Fig. 14. Force-Displacement response of TP BOR – Day 1.

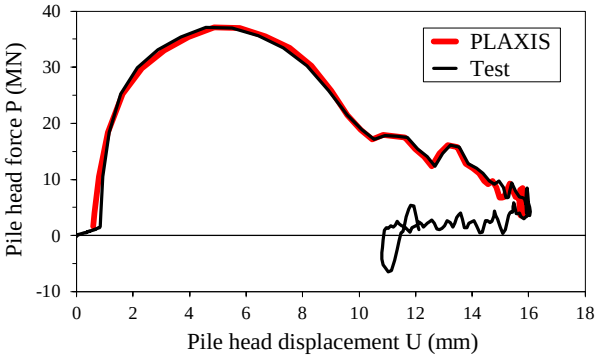

Fig. 15. Force-Displacement response of TP BOR – Day 7.

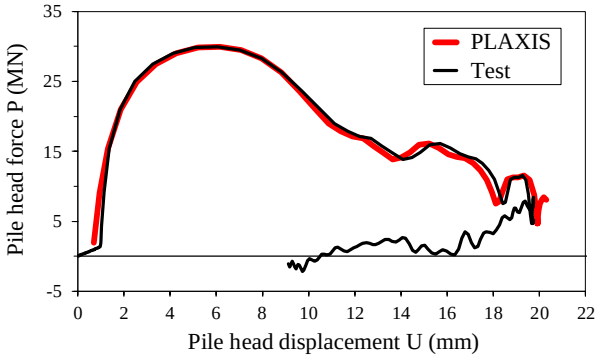

Fig. 16. Force-Displacement response of RP3 BOR – Day 29.

Note that the displacement is not measured directly in the dynamic test but rather is obtained from double integration of the acceleration time history. Therefore, numerical errors are expected to be implicit in the determination of the pile head displacement U.

6.3 Geotechnical ultimate axial resistance

The estimation of the geotechnical resistance of the pile is carried out by simulating a static test (Q-U) using the strength reduction factor of the interfaces (R_{inter}) calibrated with the high-strain dynamic test data. Since

the properties of the Soil 2 material (toe) could not be determined for the dynamic test data, the simulation of the static test is performed using the toe soil properties obtained with the calibration of the static load test data.

Figures 17, 18 and 19 plot the pile head response (Q-U) simulated with a static load test using the PLAXIS model for TP BOR - Day 1, TP BOR - Day 7, and RP3 BOR – Day 29, respectively.

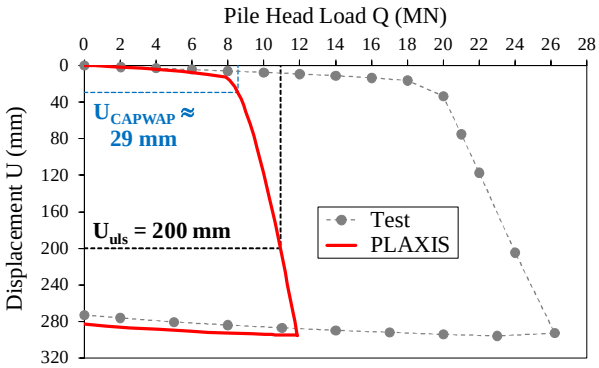

Fig. 17. Simulation of a static load test for TP BOR – Day 1.

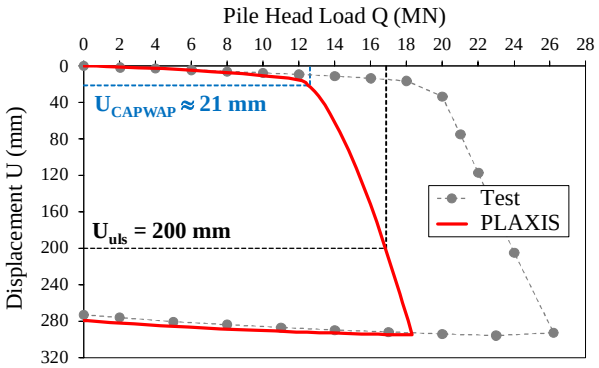

Fig. 18. Simulation of a static load test for TP BOR – Day 7.

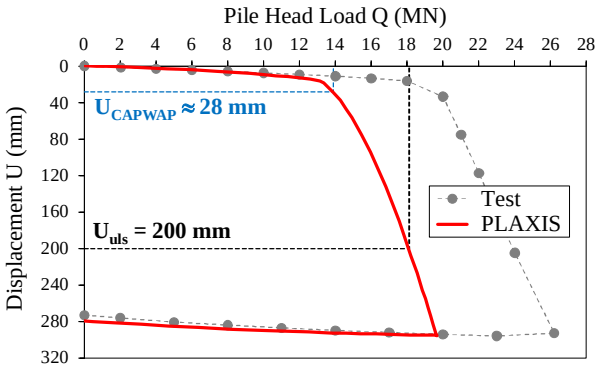

Fig. 19. Simulation of a static load test for RP3 BOR – Day 29.

The geotechnical ultimate axial resistance is obtained from the Q-U pile head response (PLAXIS) for U_{uls} = 0.1D = 200 mm. Figures 17 to 19 also indicate the pile head displacement determined by CAPWAP (U_{CAPWAP}) and the associated pile head load using the Q-U PLAXIS response. These U_{CAPWAP} displacements are about 35% to 65% higher than the peak displacements of the high-strain dynamic test because of the methodology used in CAPWAP for estimating the geotechnical resistance.

Figure 20 shows the estimation of the geotechnical axial resistance of the piles using CAPWAP (Golder 2016), PLAXIS for U = U_{CAPWAP}, and PLAXIS for U_{uls} = 0.1D = 200 mm. The geotechnical resistance obtained with the static load test on the test pile is also included for comparison.

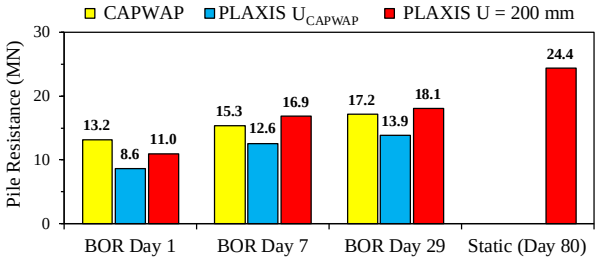

Fig. 20. Geotechnical pile resistance obtained using the high-strain dynamic and static load test data.

Figure 20 shows that the estimation of the geotechnical resistance with PLAXIS increases with the pile head displacement and with time. For instance, the increase in the resistance from U = U_{CAPWAP} (21 mm to 29 mm) to U = 200 mm is about 28% to 34%, approximately. With respect to time, the increase in the resistance for U = 200 mm from BOR Day 1 to the Static load test (Day 80 after pile installation) is about 120%. This seems consistent with the observed strength gain factor in the range of 2 or more between end of initial driving and the static load test due to soil setup for piles installed in fluvial deposits.

The estimation of the geotechnical resistance with PLAXIS for U = U_{CAPWAP} is about 18% to 35% lower than that estimated with CAPWAP, as shown in Figure 20. For the case of PLAXIS with U = 200 mm, the geotechnical resistance is about 5% to 10% higher than that estimated with CAPWAP for BOR Day 7 and 29, and about 17% lower for BOR Day 1.

Carvajal and Tara (2022a) applied the same procedure explained in this paper for 0.76 m to 1.5 m diameter, 36.5 m to 40 m embedment, open toe, driven piles installed in a fluvial deposit (sand). In that case study, the geotechnical resistance obtained with the proposed procedure was about 40% to 70% higher than that obtained with CAPWAP because of the difference in the pile head displacement to define the geotechnical resistance. However, for the 2.0 m diameter, 67 m embedment, open toe, test pile installed in the deltaic deposit (sand and silt) at the George Massey Tunnel Project, the geotechnical resistance is very similar between CAPWAP and PLAXIS U = 200 mm, even though the pile head displacements are considerably different.

Note that the estimation of the geotechnical resistance with CAPWAP depends strongly on the

analyst's experience, and the damping and quakes used for the analysis. Therefore, it is uncertain if the geotechnical resistances could have been overestimated for this large diameter, long pile for the small pile head displacement using CAPWAP.

6 CONCLUSIONS

This study reviewed the development of a procedure for estimating the geotechnical axial resistance of open-toe, steel pipe piles driven in a deltaic deposit (sand and silt) using high-strain dynamic load testing. The procedure was applied to the static and dynamic load test performed on the test pile and the reaction pile No. 3 installed for the George Massey Tunnel Replacement Project in BC, Canada.

The procedure is based on matching the work time history of the pile head obtained with the high-strain dynamic load test with that obtained using an axisymmetric finite element model. The matching procedure requires calibration of the shaft resistance and the damping of the dynamic system.

The calibration of the finite element model indicated that the dynamic response of the pile head is practically insensitive to the properties of the soil material that control the toe resistance (ϕ_{toe}, V_{s_toe}). This seems to be due to the very small displacements induced in the pile toe during the high-strain dynamic test, especially in the time interval of maximum energy transferred from the hammer to the pile.

The estimation of the geotechnical resistance of the pile is carried out by simulating a static load test (Q-U) using the strength reduction factor of the interfaces (R_{inter}) calibrated with the high-strain dynamic test data. Since the properties of the soil material that control the toe resistance could not be determined with the dynamic test data, the simulation of the static test is performed using the toe soil properties obtained with the calibration of the finite element model using the static load test data. In the absence of a static load test, the properties of the toe soil material can be assumed using the site investigation data.

The geotechnical resistance obtained with the proposed procedure and finite element model is very similar to that obtained with the 1D WEA program CAPWAP, even though the pile head displacement required to define the geotechnical resistance is significantly different between CAPWAP (21 mm to 29 mm) and PLAXIS (200 mm = 10% of the pile diameter).

REFERENCES

1) ASTM International (2017): Standard Test Method for High-Strain Dynamic Testing of Deep Foundations. ASTM D4945-17.

2) CAPWAP: Case Pile Wave Analysis Program. PDI - Pile Dynamics, Inc.

3) CSA S6-19: Canadian Highway Bridge Design Code.

4) Carvajal, JC. And Tara, D (2022a): Finite element simulation of high-strain dynamic testing of open-toe, steel pipe piles for estimation of geotechnical axial resistance. Proceedings of the 11th International Stress Wave Conference. Rotterdam, The Netherlands.

5) Golder Associates (2016): Geotechnical data report – static pile load test, George Massey tunnel replacement project (https://engage.gov.bc.ca/app/uploads/sites/52/2016/11/Highway-99-Geotechnical-Investigations-Static-Pile-Load-Test-Report-Oct-18-2016-1-Report-1.pdf)